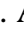# Performance Evaluation of Alkaline Activated Geopolymer Binders Using RCA and Industrial By-Products as Cement Alternatives

Mostafa Shaaban [1], Walid Fouad Edris [1, 2], Abd Al-Kader A. Al Sayed [1*], Raid S. Alrashidi [3], Tarek Ibrahim Selouma [1]

[1] Department of Civil Engineering, Giza Engineering Institute, Giza 3387722, Egypt.

[2] Department of Civil and Environmental Engineering, College of Engineering & Design, Kingdom University, Bahrain 40434, Bahrain.

[3] Civil Engineering Department, Jubail Industrial College, Royal Commission for Jubail and Yanbu, Jubail Industrial City 31961, Saudi Arabia.

Abstract

This study explores the performance of alkaline-activated geopolymer binders using industrial by-products and recycled concrete fine aggregate (RCFA) as sustainable alternatives to traditional cement. Materials such as granulated blast furnace slag (GBFS), silica fume (SF), red brick powder (RBP), quick lime (QL), and RCA were utilized to develop eco-friendly binders with enhanced mechanical and durability properties. Experimental tests evaluated physical, mechanical, and microstructural characteristics, including setting times, dry density, flexural strength, and compressive strength. Advanced analysis with SEM and EDAX examined aggregate-binder bonding. Results highlighted the critical role of binder composition in determining performance. Balanced mixtures of GBFS, SF, and RBP achieved superior strength, durability, and compact microstructures, while excessive QL increased porosity, reducing effectiveness. Optimal flexural strength (4.24 MPa at 56 days) was observed for the G30/S40-L20 formulation, underscoring the importance of precise proportions. Composition influenced setting times, with SF delaying gelation and high QL content accelerating it. The findings demonstrate the viability of using RCFA and industrial by-products in sustainable construction, offering a pathway to reduce reliance on traditional cement. The study emphasizes optimizing binder formulations for strength and durability while addressing environmental impacts, encouraging further research into long-term performance under diverse conditions. This innovative approach highlights the potential for integrating recycled and industrial by-products into construction practices to achieve eco-friendly solutions and promote sustainable urban development.

Keywords: Geopolymer; Mortar; Alkaline Activator; Recycled Concrete Fine Aggregate; Binder.

1. Introduction

Global warming is caused by the significant amount of carbon dioxide produced during the calcination process of OPC manufacture, which turns limestone into lime, and during the burning of fossil fuels to supply thermal energy for calcination [1, 2]. Energy needed for calcination, which causes global warming [3]. An estimated 0.54 tons of carbon dioxide are released during the calcination process and 0.46 tons are released as a result of burning fossil fuels for every tons of clinker produced [4, 5]. Furthermore, because geopolymers (GP) can lessen the material's environmental impact without sacrificing performance, they may eventually replace cement in shotcrete mortars [6]. Because of its advantages for the environment, alkali-activated materials have been the subject of extensive research over the past few decades [7,

8]. Alkali-activated semi-crystalline aluminosilicates, or geopolymers, are created when aluminosilicates react with alkaline media [9, 10]. Geopolymers and zeolites share a similar chemical makeup, although their microstructure is amorphous [11]. The creation of geopolymer mortar and concrete made by activating fly ash and GGBFS was the subject of numerous investigations [4, 12]. Reviews of geopolymer concrete are intended to give a thorough grasp and assessment of the material's mechanical, microstructural, physical, and mix design properties [13-15]. Inorganic polymers known as geopolymers can be amorphous or semi-crystalline [16, 17]. They are created by chemical interactions with aluminosilicate materials such fly ash, metakaolin, and leftover ceramic [18]. Alkaline activated solutions, particularly sodium-hydroxide (NaOH) and sodium meta silicates ($Na_2 SiO_3$), are what trigger these reactions [18-20]. The activator employed determines the type of polymer that is made; polysialate is often produced by alkaline activation, while polyphosphosialate is produced by acid activation [18]. Furthermore, the specific structure of the polymer network is determined by its chemical composition, which contain ferro-silico-aluminate (-Fe-O-Si-O-Al-O-), silico-oxide (-Si-O-Si-O-), silico-aluminate (-Si-O-Al-O-), and alumino-phosphate (-Al-O-P-O-) [7, 8, 21]. Dissolution, direction or movement, and polycondensation make up the intricate mechanism of the geo-polymerization reaction [22]. Numerous developments in geopolymer mechanisms for different alumino-silicate minerals have been made [23]. Figures 1-a and 1-b provide the schematic representation of a generalized mechanism that was provided [24-26].
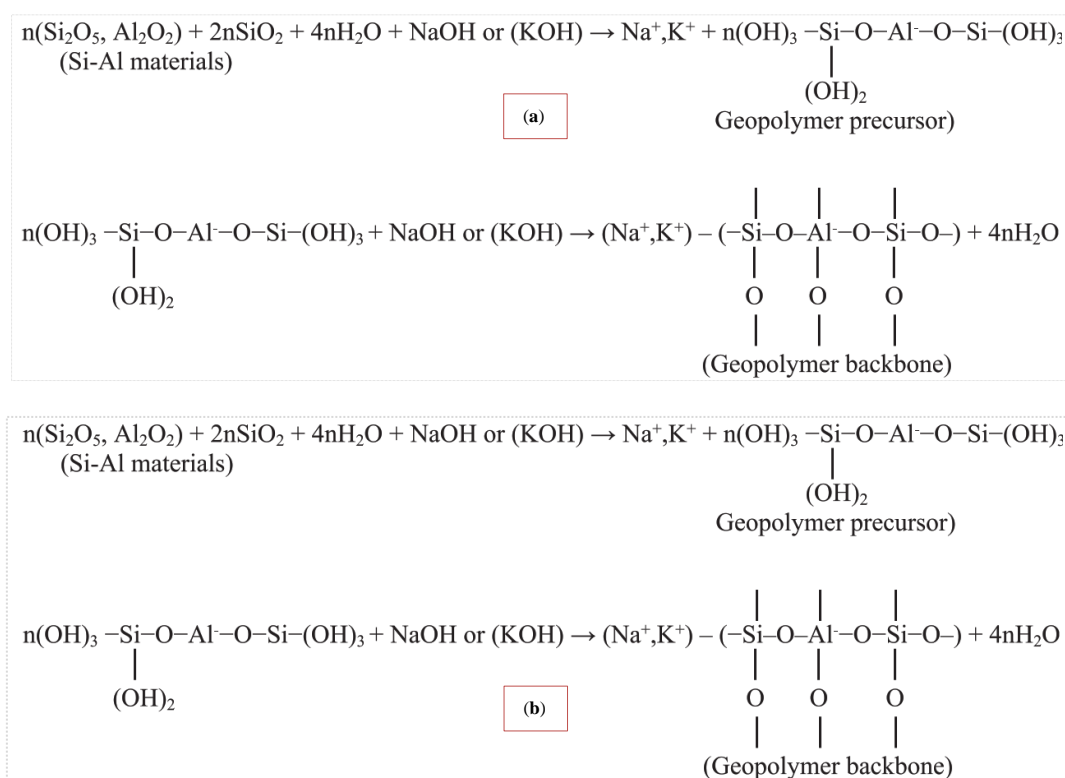

Figure 1. Chemical composition form of generalized geopolymer mechanism [1]

Rezzoug et al. [18] and Zhang et al. [21] stated that, Using ceramic sanitary-ware waste (CSW) as the only precursor, this study examined the effects of curing temperatures (60, 80, and 100 °C) and sodium hydroxide concentrations (M) of 10 and 16 on the characteristics of geopolymer mortars. Samples with higher alkali concentrations that were cured at 100 °C had the highest compressive strengths, which varied from 0.5 MPa to 11.25 MPa [21]. Increasing the alkali content reduced the porosity from 18.41% to 15.55% and increased the flowability by 16% in samples treated with 10 M and 16 M NaOH at 100 °C, respectively [18, 27]. K. Chen et al. [2, 17, 28] noted that, researchers have observed that FA-based GPs with high temperature curing exhibit superior mechanical and durability properties. However, the high temperature required for curing is not sustainable and has practical constraints [21, 29, 30]. FA-based GPs cured at room temperature have a lengthy setting time and slow strength increase at an early age due to FA's incomplete reactivity with the alkaline solution [16, 30]. Because GPs based on slag showed strong strength growth at an early age and a rapid setting time, GPs were synthesized utilizing mixes of FA and slag [18, 30, 31]. The primary goal was to create GP shotcrete utilizing cement and alkali-activated coal gasification slag aggregate [6]. A comparison was made between the efficacy of GP and cement (CM) materials for pipeline reconstruction [6]. The findings showed that GP performed better in terms of chemical resistance, cold joint removal, and environmental effect [5, 32]. The effectiveness of GP mortars applied to corrugated metal host pipes was thoroughly examined by Marathe et al. [33], who also looked into how different pipe diameters, liner thicknesses, and pre-loading circumstances affected the structural soundness of rebuilt pipe systems [6].

Yang et al. [29] demonstrated that sea sand, saltwater, and ternary solid waste were used to create marine geopolymer mortar (MGM). We looked at the fracture properties of 23 sets of MGM samples with varying alkali levels, volume fractions of marine cement mortar (MCM), and basalt fiber (BF) and polypropylene fiber (PPF). According to Tejas & Pasla [34], keeping the alkali concentration between 4 and 5 percent is recommended. Hybrid fibers showed superior overall toughness augmentation, increasing K, GF, and FBI by 54.3%, 95.6%, and 427.4%, respectively. This enhancement resulted from the synergistic action of BF and PPF, which raised the specimen's elastic modulus, decreased the speed at which cracks propagated, and maintained its ability to support loads while the crack developed [34, 35].

Matsimbe et al. [5] stated that the alkaline activator ($NaOH+Na_2SiO_3$) and the binary powder precursor (fly ash + phosphor-gypsum) reacted to form the geopolymer. Different weight percentages of phosphor-gypsum (10%, 20%, 30%, 40%, and 50%) were used in place of fly ash [5]. Based on ASTM standards, XRF, XRD, SEM-EDS, ANOVA, and Python, experimental testing and analysis were conducted [5]. According to the findings, FPGP's workability ranged from 185 to 112 mm, whereas FPGM's ranged from 145 to 100 mm [5]. The start and final setting times for the FPGP and FPGM were significantly shorter, ranging from 18 to 37 minutes and 81 to 155 minutes, respectively, and from 14 to 29 minutes and 67 to 142 minutes [5, 12]. Whereas FPGM's compressive strength ranged from 9.5 MPa to 43.27 MPa, FPGP's ranged from 7.3 MPa to 27.24 MPa [12, 36].

Ardhira et al. [9] developed the proportion of the geopolymer mix utilizing fly ash, ground granulated blast furnace slag (GGBFS), sugarcane bagasse ash (SCBA), or rice husk ash (RHA) as the primary precursor material. For a period of 365 days, the workability and mechanical characteristics of various mortar mixes containing varying percentages of RHA and SCBA were assessed [37]. With 10% SCBA and 5% RHA, geopolymer mortar improved its compressive strength by 25 percent and 13.91 percent, its flexural strength by 10.6 percent and 3.5 percent, and its split tensile strength by 35 percent and 16.8 percent, respectively [37]. The SCBA mortar SEM images clearly show good geopolymer gel formation [34, 37-39].

According to the findings by Mohammdinia et al. [27], Calcium nitrate decreased setting time and enhanced flowability. Adding 0.5–7% calcium nitrate increased mechanical strength but reduced transport properties, whereas adding 10% calcium nitrate had adverse effects. It is possible to decrease drying shrinkage and the pace at which strength declines as a result of water curing by using calcium nitrate (0.5–7%) [27]. Also, Nikmehr et al. [40] stated that, when compared to mixes that included 100% Metakaoline (MK), date palm ash (DPA) significantly enhanced the mechanical characteristics both at room temperature and after exposure to 600°C. SEM research showed that the addition of DPA to the mortar resulted in structural changes in the geopolymer mortar that could be connected to the production of a dense and packed matrix because the source materials contained highly reactive silica and alumina [40]. Hassani & Kazemian [41] examined how the characteristics of GGBS-based geopolymer mortar are affected by red mud (RM) content, curing temperature, and alkaline solution concentrations. According to the results, a major constraint of GGBS-based geopolymer mortars may be addressed by substituting RM, which may lengthen the mortars' setting time [42]. On the other hand, mortar workability decreases as RM content rises [42].

Reddy et al. [38] stated that RM significantly reduces fluidity. Additionally, GGBS enhances mechanical properties and decreases setting time. The higher GGBS content increases the geopolymer mortar's flexural and compressive strengths by providing the matrix with more CaO and creating more compact C-S-H gel [11, 21, 43]. When the GGBS blending quantity is 50% and the NaOH content is 10 M, the mortar's flexural and compressive strengths can reach 15.66 MPa and 69.06 MPa, respectively [43].

1.1. Research Significance

By utilizing industrial by-products such as granulated blast furnace slag (GBFS), silica fume (SF), red brick powder (RBP), quick lime (QL), and recycled concrete aggregate (RCA) as fine aggregate, this research explores a viable alternative to conventional Portland cement. The production of Portland cement is a major contributor to greenhouse gas emissions and resource depletion. Thus, replacing it with geopolymer binders offers a pathway to reducing the carbon footprint of the construction industry.

The incorporation of RCA into the binder not only diverts waste from landfills but also aligns with circular economy principles by reusing demolition waste. Furthermore, the use of GBFS, SF, and RBP leverages industrial by-products that are often underutilized, enhancing their value while minimizing waste.

The study's focus on assessing the material's mechanical qualities, durability, and microstructural features guarantees a thorough comprehension of its performance and opens the door for its real-world use in building. By proving that these geopolymer binders are feasible, the study meets important industry demands for long-lasting, high-performing, and sustainable materials, supporting international initiatives to lessen environmental effects and advance sustainable infrastructure development.

1.2. Research Structure

This research can be structured as follows: *Introduction*, providing the study's motivation, objectives, and significance in addressing environmental challenges; *Literature Review*, summarizing past research on geopolymer binders and recycled materials; *Materials and Methods*, detailing the components (GBFS, SF, RBP, QL, and RCA), binder formulations, and experimental procedures for assessing physical, mechanical, and microstructural properties; *Results and Discussion*, analyzing key findings on setting times, mechanical strength, and microstructural observations, emphasizing the impact of balanced binder compositions; *Conclusions*, summarizing critical insights and highlighting the potential of RCA and by-products for sustainable construction; and *References*, citing relevant studies and sources. Figure 2 shows the research methodology.
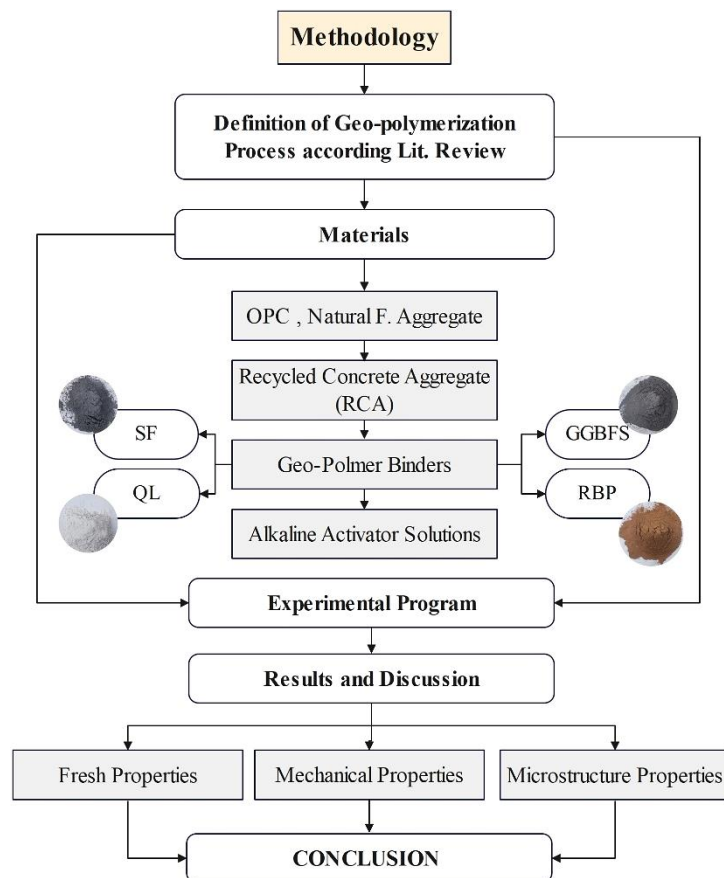

Figure 2. Research methodology

2. Materials and Methods

The performance of geopolymer binders as a fully cement substitute was evaluated in this experimental study using a variety of materials, such as ordinary Portland cement (OPC), granulated blast furnace slag (GBFS), silica fume (SF), red brick powder (RBP), quick lime (QL), natural sand, and recycled concrete aggregate. The following sections outline the properties of various materials.

Using hydrated lime $Ca(OH)_2$ as an alkaline activator, the hydraulic reactivities of the used geopolymer binders (GGBFS, SF, RBP, and QL) were assessed. In the dry condition, a solid: $Ca(OH)_2$ ratio of 80:20 was used to mix each powdered, dried solid. A 1:1 by weight mixing ratio started the hydration process. The remaining (unreacted) free lime content and the chemically mixed water content at different stages of hydration (2 and 6 hours and 1, 2, and 7 days) were measured in order to study the kinetics of hydration. Table 1 displays the amount of free lime that remains after hydration. It is evident from the results that the free lime level drops with increasing hydration time. Its use in the pozzolanic reaction with each of the substances under investigation is the cause of this decrease.

With all of the free lime being used in the first six hours of the hydration process, RBP and QL clearly showed unusually strong pozzolanic activity, which is consistent with OPC. However, after seven days of hydration, the free lime level was almost completely gone, indicating that GGBFS and SF had modest pozzolanic activity. Alkali activation is the process of combining alkaline activators with aluminosilicate source materials to start a polycondensation reaction. Activators based on sodium, such as sodium metasilicate, are essential because they supply the alkalinity required to start the reaction. As a result, the components are bound together via the creation of a three-dimensional geopolymer

network. Sodium metasilicate affects the characteristics of geopolymer cement beams by facilitating the dissolution of silica and alumina species, which encourages geo-polymerization. As a result, geopolymer cement footers have improved strength, durability, and chemical resistance, providing environmentally friendly substitutes for traditional cement-based materials.

Table 1. Remaining free lime content during hydration, where H stands for hours and d for days

Geo-polymer concrete binder	CaO, %				
	2 h	6 h	1 d	2 d	7 d
OPC	0.1	0	0	0	0
RBP	0.43	0.32	0	0	0
GGBFS	7.9	5.8	4.9	3.2	0.39
QL	8.2	6.1	1.7	0	0
SF	6.1	5.9	3.6	2.5	2.1

2.1. Aggregate

The control mix, which contained fine aggregate of natural sand, had a fineness modulus of 2.9 and a specific gravity of 2.58. The ASTM C33M [44] standard specification was met by the natural sand that was utilized. In every geopolymer mortar mix, recycled concrete aggregate (RCA), which has a specific gravity of 2.23 and a fineness modulus of 3.7, was utilized as a fine aggregate. Recycled aggregate is one long-term solution to the environmental damage caused by the construction sector. Recycled concrete aggregate (RCA) is made by crushing all concrete demolition waste. Recycled concrete aggregates contain hydrated cement paste in addition to the original ingredients. This paste reduces specific gravity and increases porosity when compared to similar virgin aggregates. Higher absorption results from RCA's increased porosity. Thus, the usual method for enhancing the RCA's qualities is to remove the adhering mortar. Old mortar on RCA surfaces may usually be removed by ball milling and crushing. To get an aggregate of the right size, the crushed pieces were then sieved. Figure 3 shows the grading curve for recycled concrete aggregate and utilized fine aggregate. Moreover, Table 2 lists these aggregates' mechanical and physical characteristics.
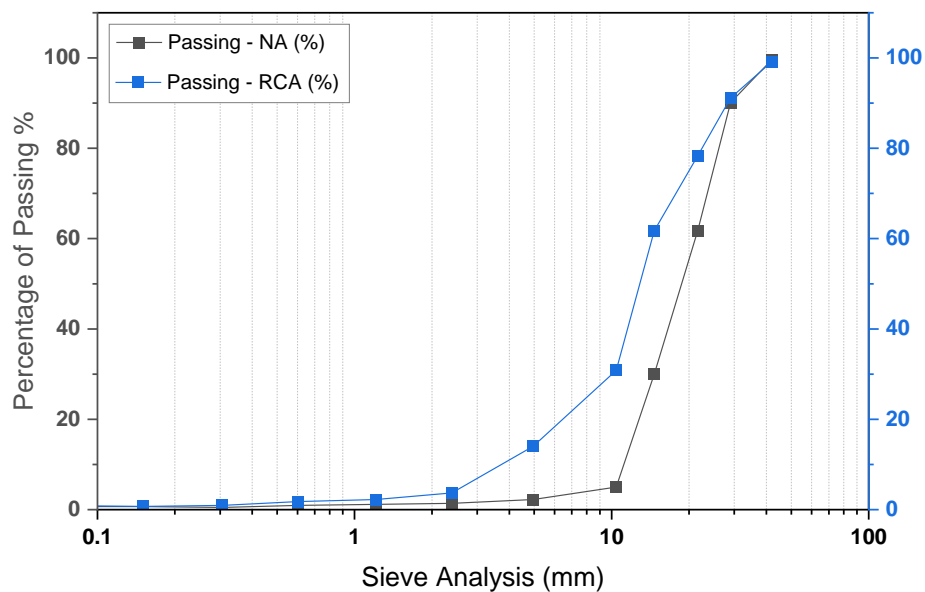
Figure 3. The grading curve for recycled concrete aggregate (RCA) and utilized fine aggregate (NA)

Table 2. Recycled concrete fine aggregate and natural sand mechanical and physical characteristics

Property	Recycled Concrete Fine Agg.	Natural Sand
Specific gravity	2.23	2.58
Volume density	1390	1612
Water absorption %	5.67	1.9
Los Angles abrasion %	25.8	-
Crushing Value %	28.4	-

2.2. Binder Materials

Throughout the study, Portland cement type I [CEM I 42.5N] with a specific gravity of 3.15 was used as binder in the control mix. The cement was selected to conform to ASTM C150/C150-M [45] standard specification. The cement alternatives used in this experiment were granulated blast furnace slag (GBFS), silica fume (SF), red brick powder (RBP), and quick lime (QL). Figure 4 shows samples of materials used as a substitute for cement.
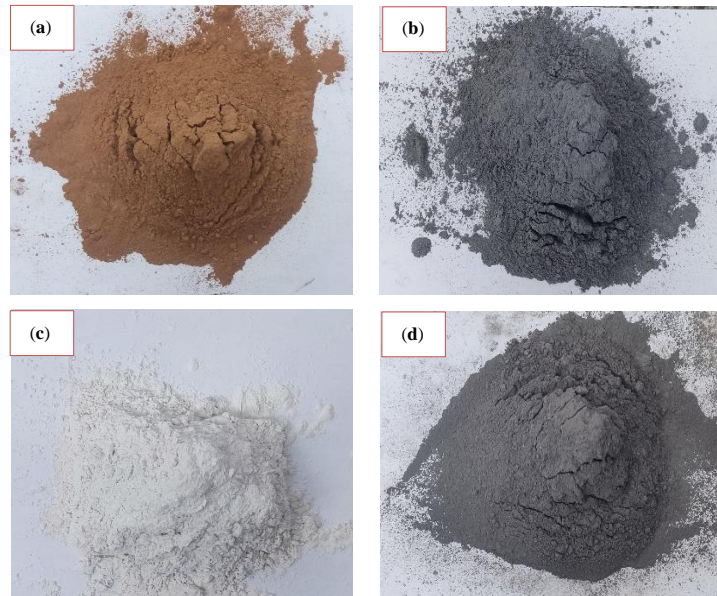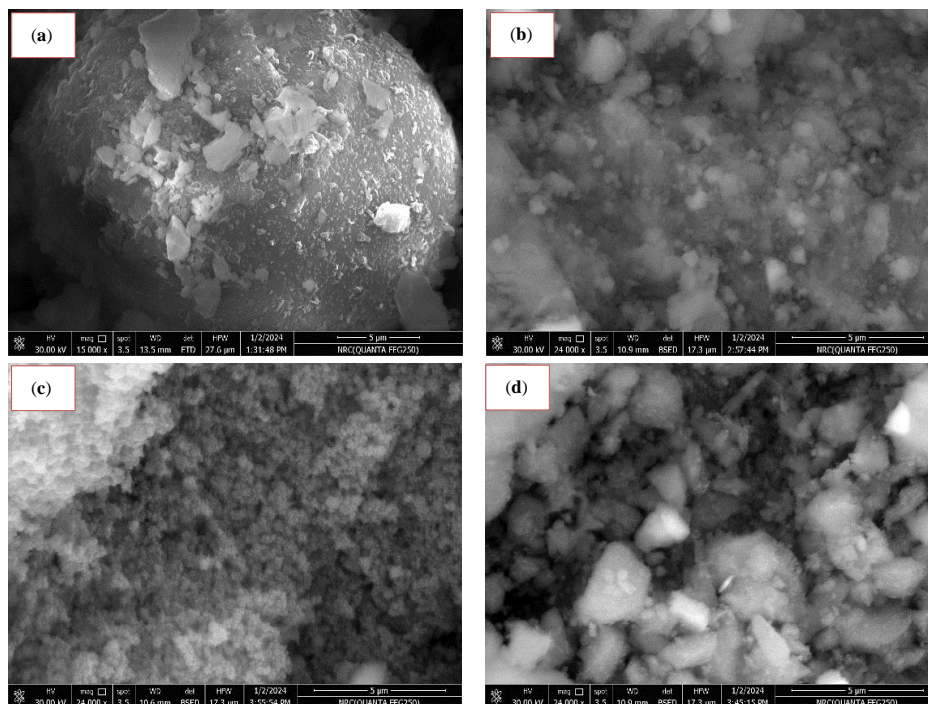

Figure 4. Samples of materials used as a substitute for cement. (a) Red brick powder (RBP), (b) Silica fume (SF), quick lime (QL), and Granulated blast furnace slag (GBFS)

The chemical composition of and physical properties of these materials are shown in Table 3. Moreover, Figures 5-a to 5-e depict the elemental composition of the utilized cementitious materials according to scanning electron microscope (SEM).

Table 3. Chemical Constituent of cementitious materials

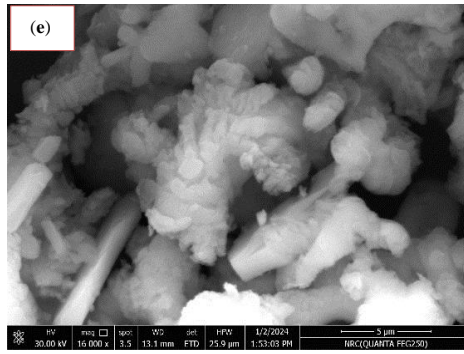| Material	Cao	SiO$_2$	Al$_2$O$_3$	Fe$_2$O$_3$	MgO	K$_2$O	LOI	Average PS - (μm)
OPC	58.1	25.5	7.37	4.16	1.76	0.7	1.7	9.9
GBFS	40.42	32.22	15.0	0.5	7.4	0.47	3.8	2.4
SF	0.8	96.5	0.5	2.0	0.9	2.0	2.9	12
RBP	7.15	51.6	14	10.4	1.67	-	1.74	25
QL	55.4	0.2	0.03	0.04	-	-	5.6	12.8

Figure 5. SEM of materials used as a substitute for cement. (a) Portland cement (RBP), (b) Granulated blast furnace slag (GBFS), (c) Silica fume (SF), (d) Red brick powder (RBP) and (e) quick lime (QL)

Also, Figures 6-a to 6-e depict the elemental composition of the utilized cementitious materials by the Energy-dispersive X-ray analysis (EDS or EDAX)
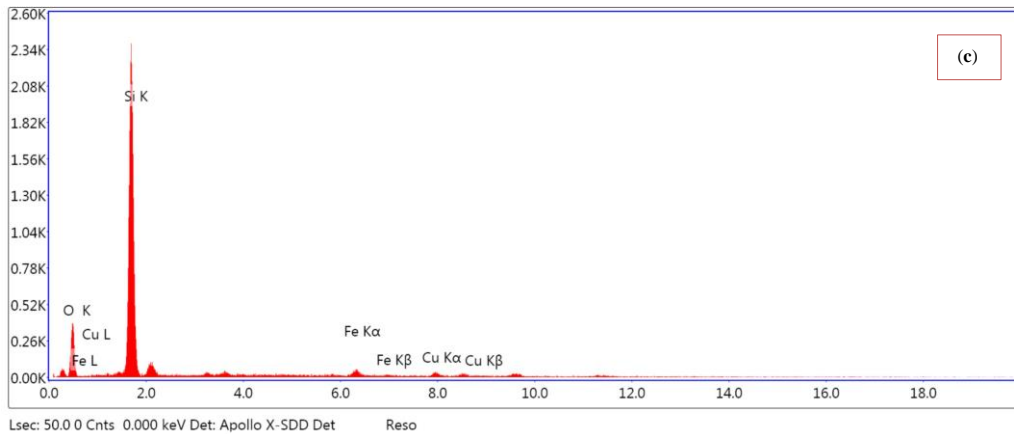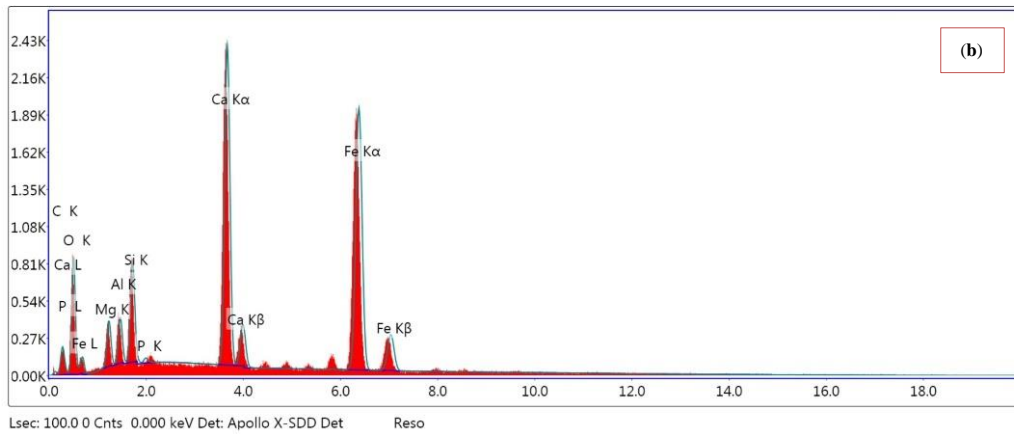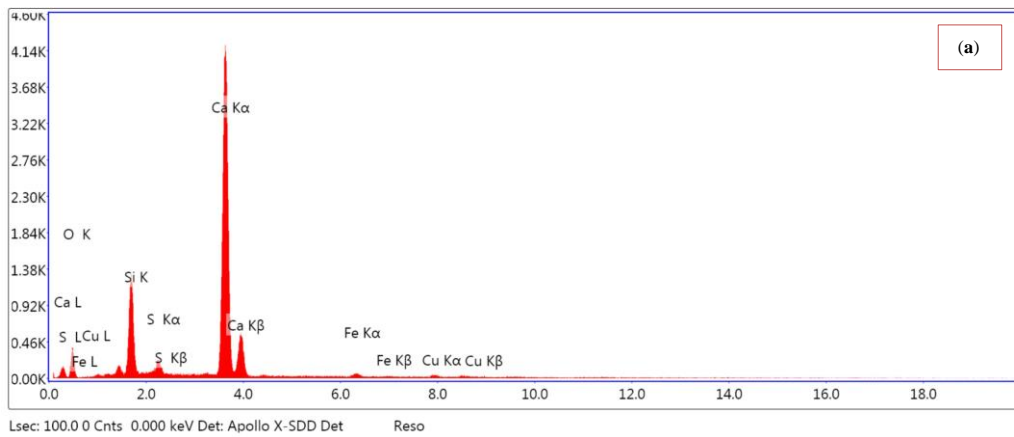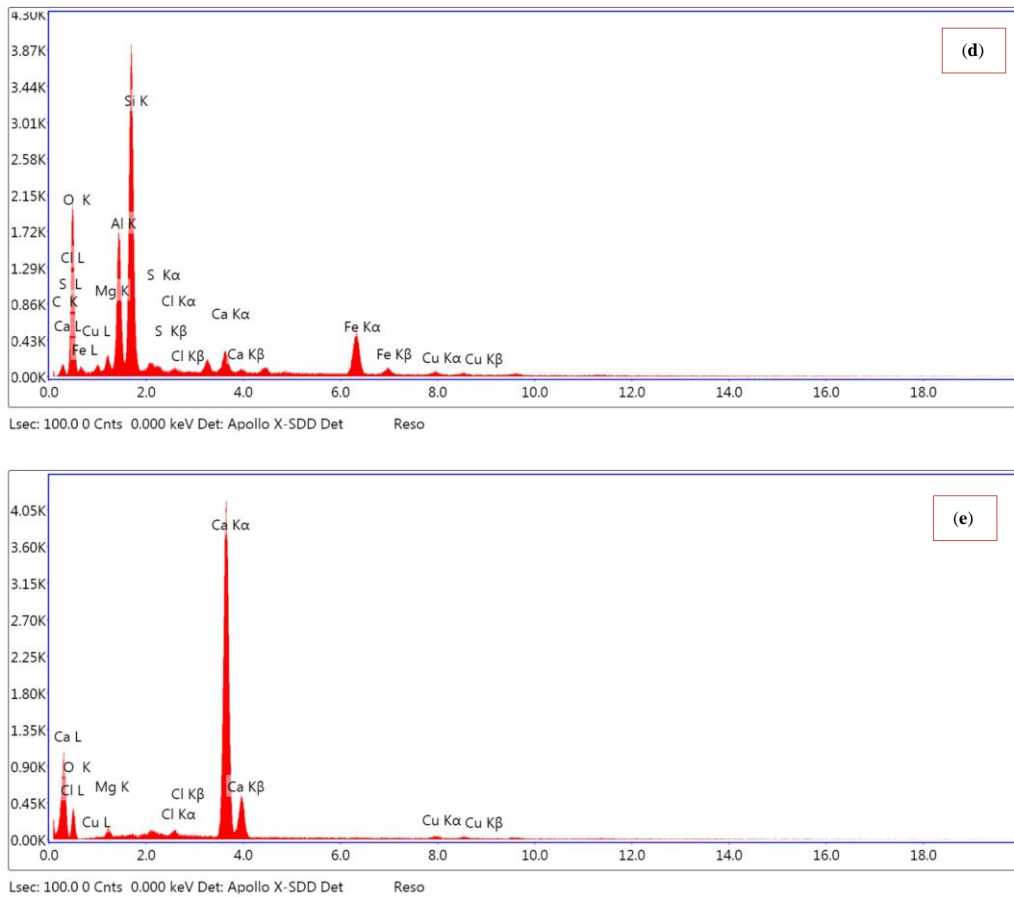
Figure 6. EDAX of materials used as a substitute for cement. (a) Portland cement (RBP), (b) Granulated blast furnace slag (GBFS), Silica fume (SF), Red brick powder (RBP), quick lime (QL)

2.3. Alkaline Activator (AA) and Water

The alkaline activator used in this study was prepared by mixing sodium hydroxide solution (NaOH) and sodium silicate liquid (Na_2SiO_3) (Figure 7) with Na_2SiO_3/NaOH ratio of 2.0 by weight. Firstly, the NaOH solution was prepared by dissolving the high purity caustic soda in distilled water to the required molarity (14 mole/L). The Alkaline Activator solution was prepared one day before casting the specimens. After mixing well, it was left to cool to room temperature. The potable water complies with ASTM C1602 [46] was used in mixing the dry materials. The water to binder ratio (W/C) was constant for all mixtures and equal to 0.35.

Figure 7. Sample of alkaline activator solutions

2.4. Mixed Proportions

To evaluate the efficacy of geopolymer binders as a fully cement alternative, six mortar mixes were prepared so that the fine aggregate-binder-water ratio was maintained at a constant 2:1:0.35 for all mixtures. The control mix contains 100% (OPC) was prepared, in addition to ten geopolymer mixtures with 0% (OPC). The control mix contains fine aggregate of natural sand, whi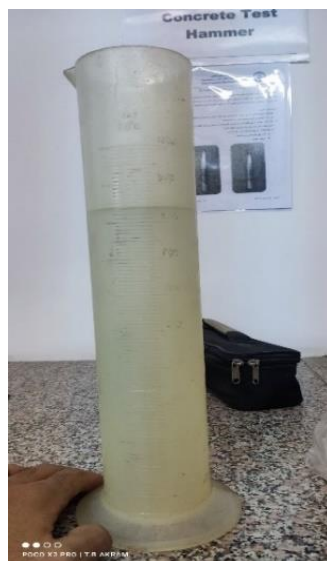le the geopolymer mixes contain recycled concrete aggregate as fine aggregate. In the geopolymer mixes, constant proportions of red brick powder (10%), ground granulated blast furnace slag (GBFS) (30%), and variable proportions of silica fume and lime were used. The alkaline activator was blended with binders into a ratio (AA/Binder) of 0.44. The details for each mix proportion are presented in Table 4, where the control mix is denoted by C, while mixes containing geopolymer binder are denoted by GSL.

Table 4. Mix designs of Mortars (Kg/m³)

Mix designation	Fine aggregate		Cementitious Materials					Water	NaOH sol.	Sodium Silicate
	Sand	RCA	Opc	GGBFS	RBP	SF	QL			
C₀	1612	--	800	--	--	--	--	280	--	--
GB/S60-L0						420	0			
G30/S50-L10						350	70			
G30/S40-L20						280	140			
G30/S30-L30	--	1390	--	210	70	210	210	245	103	206
G30/S20-L40						140	280			
G30/S10-L50						70	350			
G30/S0-L60						0	420			

2.5. Methods

To create a homogenous fresh mortar, the dry ingredients were first added to the mixer and mixed for two minutes. Next, the alkali activator was added, and last, water was added in the appropriate amounts. The prepared fresh mortars were poured into standard molds, twenty-four hours after casting; the specimens were removed from molds and stored at laboratory temperature and a humidity of 95%, protected from water evaporation using plastic sheet. Subsequent tests were conducted based on the corresponding standard specifications to evaluate the performance of the geopolymer mortar.

2.5.1. Fresh Properties

For setting Time, the initial and final setting times of the fresh pastes were determined using a Vicat apparatus (Figure 8), following the guidelines of ASTM C191 [47]. Also, the fluidity of the fresh mortar was assessed using the Flow Table test, conducted in accordance with ASTM C1437-20 [48].

Figure 8. Initial and final setting times apparatus

2.5.2. Hardened Properties

Tests for compressive strength, dry unit weight, flexural strength, and linear shrinkage were conducted in order to assess the hardened properties of the mortars under investigation.

Compressive Strength Test

This test was conducted on cubic specimens measuring (70 × 70 ×70 mm), in accordance with ASTM C109 [49]. The specimens were demolded 24 hours after casting and then cured in water for 7, 28, and 56 days. Figures 9-a and 9-b shows the cubes samples in standard molds and after demold, respectively.

Figure 9. Casted samples used in compressive strength

Flexural Strength Test

In accordance with ASTM C348-21, this test was conducted on specimens that measured 160 x 40 x 40 mm after curing for 7, 28, and 56 days [50].

Dry Density

Determination of dry bulk density of hardened mortar calculated by adapting the Standard: BS EN 1015-11 [51]. The mean dry density of the three samples is required to be recorded for 7, 28, and 56 days to the nearest 10 kg/m^3. The oven shown in Figure 10 was used to dry the samples while measuring process of the dry density.

Figure 10. Electric oven used in drying process

Microstructure Characterization

Microstructure characterization After testing the compressive strength at 56 days, part of the crushed samples was dried for scanning electron microscopy (SEM) analyses conducted with to obtain the microstructure of the geopolymer mortar.

3. Results

3.1. According to Fresh Properties

Both of Table 5 and Figure 9 shows how the amount of used alternative Cementous materials affects the new characteristics of geopolymer binders setting times. With constant percentage of both red brick powder (10%), granulated blast furnace slag (GBFS) (30%), NaOH molarity (14 mole/L) and Na2SiO3/NaOH ratio of 2.0, it is evident that the initial setting time decreased when the QL content increased from 0% to 60%.

Table 5. Setting times different mortars mixtures (min.)

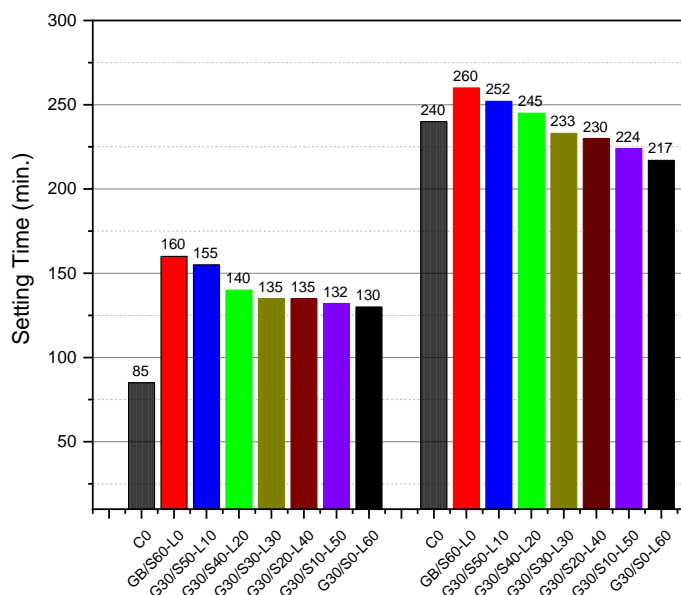| Mix designation	Setting Time - (min.)		Flow – (mm)
	Initial	Final	
C$_0$	85	240	192
GB/S60-L0	160	260	185
G30/S50-L10	155	252	180
G30/S40-L20	140	245	174
G30/S30-L30	135	233	168
G30/S20-L40	135	230	163
G30/S10-L50	132	224	157
G30/S0-L60	130	217	152

Figure 11. Initial and final setting time (min.) for different blended geopolymer mortar mixtures

The initial and final setting times of the geopolymer binders demonstrate notable trends when compared to the Control sample, which had the shortest setting times (initial: 85 minutes; final: 240 minutes). This Control mixture, representing conventional binders, displayed faster setting due to the rapid hydration reactions typical of ordinary Portland cement (OPC). In contrast, all other mixtures, incorporating combinations of granulated blast furnace slag (GBFS), silica fume (SF), red brick powder (RBP), quick lime (QL), and recycled concrete aggregate (RCA), exhibited extended setting times.

The highest initial and final setting times were observed in the GB/S60-L0 mixture (initial: 160 minutes; final: 260 minutes). This can be attributed to the high SF content, which is known for slower reaction kinetics compared to OPC due to its reliance on alkaline activation and calcium silicate hydrate (C-S-H) gel formation. Studies confirm that slag's slower dissolution delays the binding process, resulting in prolonged setting times. As the QL content increased in subsequent mixtures (e.g., G30/S0-L60, with 60% QL), both the initial (130 minutes) and final (217 minutes) setting times decreased. Quick lime enhances the alkalinity of the mixture, which accelerates the dissolution of aluminosilicate phases and promotes faster geopolymer gelation. This finding aligns with previously published research indicating that higher lime content improves reaction rates, leading to reduced setting times. The

gradual decrease in setting times from GB/S60-L0 to G30/S0-L60 also reflects the diminishing influence of silica fume. SF slows the geo-polymerization process by requiring extended dissolution periods for its reactive silica, as supported by existing studies.

In conclusion, the highest setting times were recorded for GB/S60-L0, while the lowest were observed for G30/S0-L60, highlighting the role of material composition in tailoring setting behavior.

Also, according to Table 4 and Figure 12, the flow test results indicate a gradual decrease in the workability of mortar mixtures as the material composition transitions from the Control sample to mixtures with higher quick lime (QL) content and reduced silica fume (SF) proportions. The flow values ranged from 192 mm for the Control sample to 152 mm for the G30/S0-L60 mixture, representing the highest and lowest flow values, respectively.
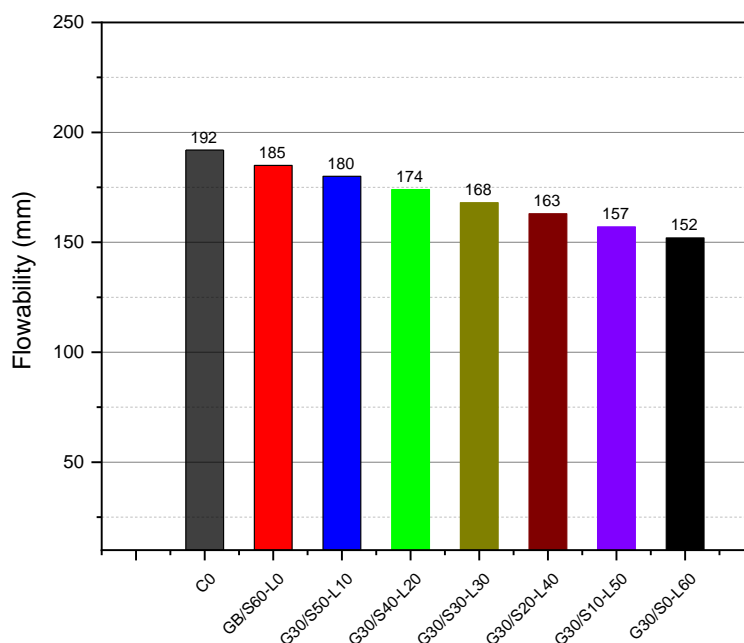

Figure 12. Flowability (mm) for different blended geopolymer mortar mixtures

The Control mixture, composed of ordinary Portland cement (OPC), exhibited the highest flow (192 mm), reflecting the superior workability provided by OPC due to its uniform particle size distribution and low water demand for adequate flow. As geopolymer materials were introduced, a reduction in flow was observed, beginning with GB/S60-L0 (185 mm) and decreasing progressively in subsequent mixtures. The decline in flow corresponds with increasing QL content and decreasing SF content. Also, the mixture G30/S0-L60, which contained the highest QL proportion (60%), exhibited the lowest flow value (152 mm). The addition of QL significantly increased the alkalinity of the mixture, promoting rapid geopolymer gelation and reducing free water availability for flow. Previous studies confirm that higher lime content accelerates geo-polymerization, resulting in reduced workability. Similarly, the reduction in SF content also contributed to the lower flow values, as SF is known for its fine particle size and smooth surface, which improve lubrication in mortar mixtures [5, 17]. Reduced SF content thus diminishes these benefits, leading to lower workability.

In summary, the highest flow (192 mm) was achieved by the Control sample, while the lowest (152 mm) was observed in G30/S0-L60. This variation highlights the significant influence of material composition, particularly QL and SF proportions, on the flow characteristics of geopolymer mortars.

3.2. According to Dry Density

According to Table 6 and Figure 13, the dry density results of mortar samples after 7 days reveal a clear trend influenced by the incorporation of geopolymer materials and varying proportions of granulated blast furnace slag (GBFS), silica fume (SF), and quick lime (QL). The Control sample recorded the highest dry density of 2.16 g/cm³, while the lowest density, 1.81 g/cm³, was observed for the GB/S60-L0 mixture. The variations in dry density are primarily attributed to differences in material composition and particle packing efficiency.

Table 6. Dry density of for different blended geopolymer mortar mixtures (gm/cm³)

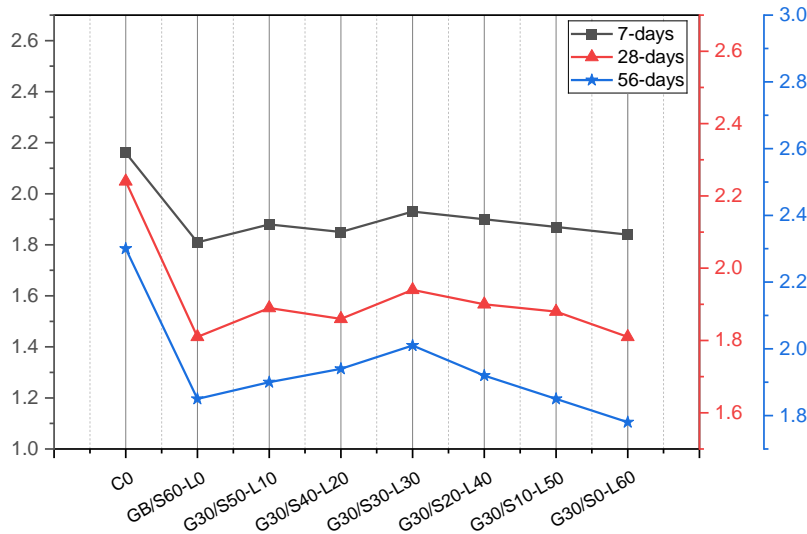| Mix designation	Dry Density – (gm/cm³)		
	7 - days	28 - days	56 - days
C_0	2.16	2.24	2.3
GB/S60-L0	1.81	1.81	1.85
G30/S50-L10	1.88	1.89	1.90
G30/S40-L20	1.85	1.86	1.94
G30/S30-L30	1.93	1.94	2.01
G30/S20-L40	1.90	1.90	1.92
G30/S10-L50	1.87	1.88	1.85
G30/S0-L60	1.84	1.81	1.78

Figure 13. Dry Density (gm/cm³) for different blended geopolymer mortar mixtures at 7, 28 and 56 days

The control sample, composed entirely of OPC, exhibited the highest density due to the dense microstructure and hydration products formed by OPC. In contrast, the GB/S60-L0 mixture, which lacks SF and has a high GBFS content, showed a significant density reduction (16.2% lower than the control sample). This reduction can be attributed to the porous nature of GBFS, which limits the compactness of the geopolymer matrix [1, 17].

As SF and QL were introduced, the dry density increased slightly. For instance, the G30/S30-L30 mixture recorded a density of 1.93 g/cm³, approximately 10.6% lower than the control. SF contributes to improved packing density due to its ultrafine particles, which fill voids within the matrix. However, excessive QL content in mixtures like G30/S0-L60 resulted in marginally reduced density (1.84 g/cm³) due to increased porosity caused by rapid reaction and incomplete gel formation.

In conclusion, the highest density was observed in the control sample (2.16 g/cm³), and the lowest in GB/S60-L0 (1.81 g/cm³). The variations in density highlight the influence of geopolymer composition on matrix compactness and porosity, aligning with findings from similar studies on geopolymer materials. Also, the dry density of mortar samples after 28 and 56 days shows variations influenced by the incorporation of industrial by-products and alkaline-activated recycled concrete aggregate (RCA). These variations reflect the influence of geopolymer binder composition on the microstructure and packing density of the mortar. At 28 days, the control sample achieved the highest density (2.24 g/cm³), attributed to the dense hydration products of OPC. In comparison, the GB/S60-L0 mixture recorded the lowest density (1.81 g/cm³), a 19.2% reduction relative to the control. This decrease is due to the lower hydration reaction of GBFS as a primary binder, leading to a more porous matrix [1, 13, 19].

By 56 days, the control sample further increased in density to 2.3 g/cm³, demonstrating continued hydration and matrix densification. Mixtures incorporating silica fume (SF) and quick lime (QL) showed progressive improvements in density. For example, G30/S30-L30 reached 1.94 g/cm³ at 28 days and increased to 2.01 g/cm³ at 56 days (an 8.3% improvement compared to 28-day density). SF's ultrafine particles enhance particle packing and matrix compactness,

while QL contributes to accelerated geo-polymerization. However, mixtures with excessive QL, such as G30/S0-L60, showed reduced density at 56 days (1.71 g/cm³, the lowest value), due to excessive porosity caused by rapid reaction and incomplete gel formation.

The increase in density from 28 to 56 days across all mixtures highlights ongoing geo-polymerization and matrix refinement over time. For instance, G30/S40-L20 showed a 4.3% increase (from 1.86 g/cm³ to 1.94 g/cm³). This trend aligns with the prolonged pozzolanic reactions and densification typical of geopolymer binders. The highest density at 56 days was observed in the control (2.3 g/cm³) and G30/S30-L30 (2.01 g/cm³), while the lowest was in G30/S0-L60 (1.71 g/cm³). These findings indicate that a balanced combination of GBFS, SF, and QL enhances the density and structural integrity of geopolymer mortars over time.

3.3. Compressive Strength

Firstly, Figure 14 shows the compressive strength test applied for one of the cast cube samples, explaining the failure behavior of most tested cubes. Also, according to Table 7 and Figure 15, the compressive strength results for mortar samples after 7 days show varying trends based on the proportions of alkaline activators and industrial by-products, demonstrating the influence of material composition on strength development. The control mixture exhibited a compressive strength of 32.3 MPa, serving as the benchmark for comparison. The lowest strength was observed in GB/S60-L0 (27.3 MPa), representing a 15.5% reduction compared to the control. This decrease is primarily due to the insufficient reactivity of granulated blast furnace slag (GBFS) without adequate activators, resulting in slower geo-polymerization [52, 53]. In contrast, G30/S40-L20 achieved the highest compressive strength (36.1 MPa), reflecting an 11.8% increase relative to the control. The optimized balance of silica fume (SF) and quick lime (QL) in this mixture enhanced the early-age geo-polymerization process and binder matrix densification [5, 32]. It's noticed that the highest compressive strength was obtained for G30/S40-L20 (36.1 MPa), while the lowest compressive strength was recorded for GB/S60-L0 (27.3 MPa).

Figure 14. Compressive strength test (one of the samples during the test)

Table 7. Compressive strength in (MPa) and Flexural strength in (MPa) for different blended geopolymer mortar mixtures

| Mix designation	Compressive strength – (MPa)			Flexural strength – (MPa)		
	7 - days	28 - days	56 - days	7 - days	28 - days	56 - days
C₀	32.3	43.8	47.5	3.45	4.3	4.75
GB/S60-L0	27.3	35.21	38.91	3.1	3.52	3.7
G30/S50-L10	35.2	45.42	49.8	3.52	4.1	4.2
G30/S40-L20	36.1	46.47	51.15	3.56	4.1	4.24
G30/S30-L30	35.49	45.78	50.3	3.53	4.03	4.21
G30/S20-L40	31.95	41.2	45.11	3.35	3.8	3.87
G30/S10-L50	31.10	٤٠.17	43.90	3.21	3.65	3.71
G30/S0-L60	29.85	38.55	41.86	3.19	3.53	3.70
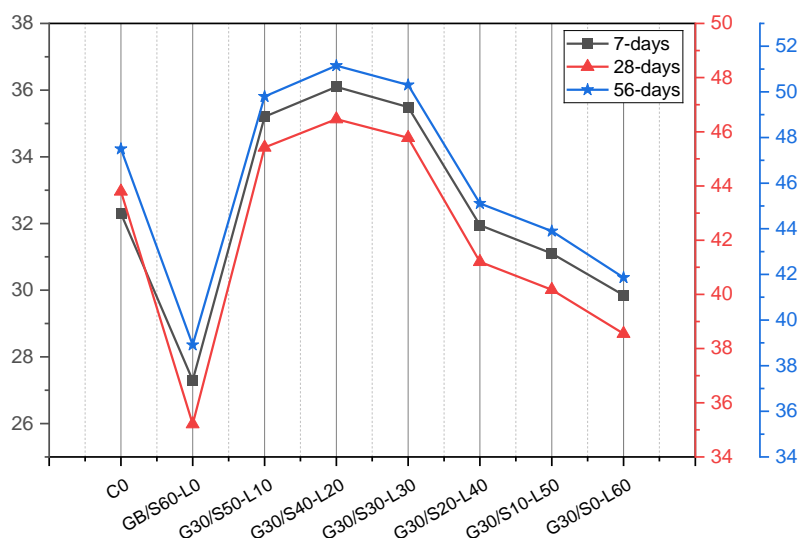
Figure 15. Compressive strength (MPa) for different blended geopolymer mortar mixtures at 7, 28 and 56 days

The enhanced compressive strength of G30/S40-L20 is attributed to silica fume's ability to improve particle packing and pozzolanic activity, resulting in a denser and more robust matrix. Quick lime contributes calcium ions, which accelerate geopolymer gel formation and improve structural integrity [13, 54]. However, excessive QL content in G30/S0-L60 (29.85 MPa) reduced strength due to microcracking caused by rapid reactions. The results emphasize the importance of balancing industrial by-products and activators to optimize compressive strength. G30/S40-L20 demonstrated the best performance, highlighting the effectiveness of combining SF and QL.

The compressive strength results for mortar samples after 28 and 56 days demonstrate significant variations influenced by the mix proportions of granulated blast furnace slag (GBFS), silica fume (SF), red brick powder (RBP), quick lime (QL), and recycled concrete aggregate (RCA). These variations highlight the impact of material selection on strength development in geopolymer systems.

At 28 days, the control mixture achieved 43.8 MPa. The lowest compressive strength was observed in GB/S60-L0 (35.21 MPa), a 19.6% reduction, due to limited reactivity of GBFS when used alone, as noted in earlier studies (Xu & van Deventer, 2000). The highest strength was found in G30/S40-L20 (46.47 MPa), a 6.1% increase, attributed to the optimized balance of SF and QL, which enhanced geopolymer gel formation and matrix densification (Davidovits, 2008). While at 56 days, the control mixture showed 47.5 MPa. GB/S60-L0 remained the lowest (38.91 MPa, a 18.1% reduction), while G30/S40-L20 reached the highest (51.15 MPa, a 7.7% increase). This increase is consistent with the ongoing geo-polymerization process over time [14, 35].

The superior performance of G30/S40-L20 is linked to silica fume's enhanced pozzolanic activity, contributing to a denser and more durable matrix. Quick lime provides additional calcium ions, promoting stronger calcium-silicate-hydrate (C-S-H) and geopolymer gels. The reduction in strength for GB/S60-L0 is due to the lack of sufficient silica and calcium sources to sustain effective geo-polymerization. The results demonstrate that mixtures with balanced proportions of SF and QL outperform the control, particularly G30/S40-L20, which exhibited superior long-term strength. These findings emphasize the need for careful material optimization in geopolymer systems.

The superior performance of G30/S40-L20 can be attributed to the synergistic effects of silica fume's enhanced pozzolanic activity and the optimal presence of quick lime. Silica fume, with its high specific surface area and amorphous silica content, reacts with calcium hydroxide to form additional calcium-silicate-hydrate (C-S-H) gel, significantly densifying the matrix. This densification improves the bonding between the aggregate and binder phases, reducing porosity and enhancing overall durability. Quick lime acts as a supplementary activator by providing an abundant source of calcium ions, which further react with silica and alumina to promote the formation of robust geopolymer gels and C-S-H phases, as supported by previous studies. The resulting matrix demonstrates superior mechanical performance and long-term strength, as observed in G30/S40-L20.

In contrast, the GB/S60-L0 mixture exhibits reduced compressive strength due to the absence of sufficient reactive silica and calcium sources necessary for effective geo-polymerization. Without these critical components, the development of a cohesive matrix is hindered, leading to increased porosity and weaker structural integrity. This highlights the limitations of relying solely on GBFS without supplementary pozzolanic or calcium-rich materials.

The findings emphasize that balanced proportions of silica fume and quick lime are critical to optimizing the compressive strength of geopolymer binders. Mixtures like G30/S40-L20 not only outperform the control but also

maintain superior strength over time. This underscores the importance of material optimization to achieve a dense microstructure and robust mechanical performance in geopolymer systems. Such optimization ensures sustainable and high-performing alternatives to traditional cementitious materials.

3.4. Flexural Strength

Depending on the mix composition as illustrated in Table 6 and Figure 16, the mortar samples' flexural strength after seven days varies. In addition to the usage of recycled concrete aggregate (RCA) as fine aggregate, the results show the impact of binder ingredients such granulated blast furnace slag (GBFS), silica fume (SF), red brick powder (RBP), and quick lime (QL).
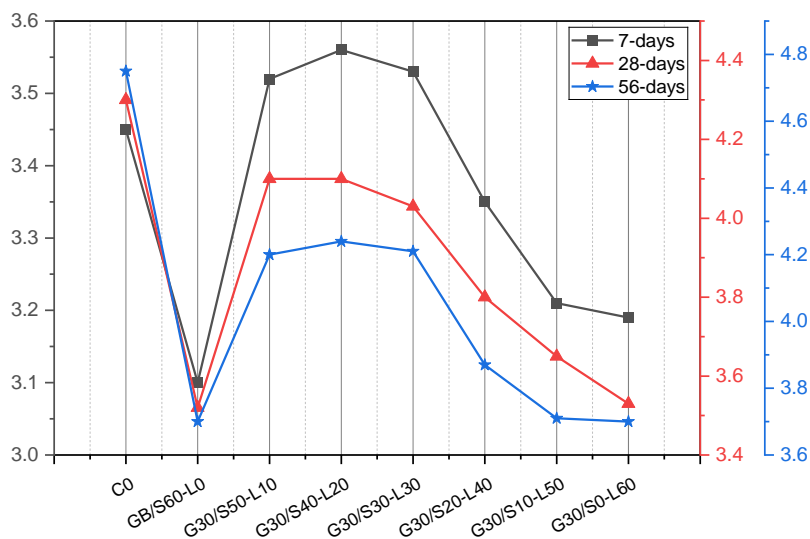

Figure 16. Flexural strength (MPa) for different blended geopolymer mortar mixtures at 7, 28 and 56 days

The mix G30/S40-L20 achieved 3.56 MPa, surpassing the control by 3.2%. This increase can be attributed to the balanced proportions of silica and alumina provided by SF and RBP, which promote denser geopolymer matrices and stronger interfacial bonding. The mix G30/S0-L60 yielded 3.19 MPa, a 7.5% reduction compared to the Control. This reduction is due to the high quick lime content, which may result in excessive shrinkage and microcracking during curing, as noted by Anju et al. [52]. The increased flexural strength in mixes like G30/S40-L20 is attributed to effective geo-polymerization facilitated by the synergistic interaction of GBFS, SF, and QL. The higher reactivity of these components leads to the formation of a compact matrix with enhanced tensile resistance. Conversely, reduced flexural strength in mixes with higher QL content, such as G30/S0-L60, reflects a compromised microstructure due to the potential for lime-induced porosity and cracking, aligning with findings from Poornima et al. [3] and Hassani & Kazemian [41]. While the control mix displayed robust flexural strength, G30/S40-L20 demonstrated a slight improvement, highlighting the potential for optimizing geopolymer binder compositions. The lowest values underline the necessity of carefully balancing lime content to mitigate adverse effects on the mortar's structural integrity.

As shown in Table 6, it showed that at 28 days, the control mixture achieved 4.3 MPa. The lowest flexural strength was observed in GB/S60-L0 (3.52 MPa), an 18.1% reduction, due to the limited formation of polymeric chains from GBFS alone, as indicated in studies by Poornima et al. [3] and Hassani & Kazemian [41]. G30/S50-L10 and G30/S40-L20 both achieved 4.1 MPa, a 4.7% reduction, attributed to their balanced content of SF and QL, which facilitated better microstructural cohesion. On the other hand, at 56 days, the control mixture improved to 4.75 MPa. GB/S60-L0 remained the lowest (3.7 MPa, a 22.1% reduction). G30/S40-L20 achieved the highest (4.24 MPa, an 11% reduction compared to the control), demonstrating that silica and calcium synergy contributed to enhanced tensile performance over time.

Flexural strength results reveal that incorporating SF and QL optimizes the geopolymer matrix by increasing the interfacial bond between fine aggregates and the binder, enhancing tensile resistance. However, lower flexural strength in GB/S60-L0 can be linked to the insufficient reactive silica and alumina content, which limits geo-polymerization efficiency [29, 35]. RCA as fine aggregate may have slightly reduced flexural strength due to higher porosity and weaker interfacial transition zones [22]. While the control mixture showed the highest flexural strength, the G30/S40-L20 mix demonstrated competitive performance, emphasizing its potential as a sustainable alternative with adequate tensile capacity. The data also underline the importance of optimizing mix proportions to achieve improved strength characteristics.

3.5. Microstructure Properties

The SEM analysis provides insights into the microstructural characteristics of the mortar samples prepared with alkaline-activated geopolymer binders. The morphology, compactness, and presence of microcracks or voids in the samples vary based on the binder composition. For GB/S60-L0 sample, Figure 14-a shows a porous structure with noticeable voids, attributed to insufficient geo-polymerization due to the limited silica and alumina content. Figures 14-b and 14-c show G30/S50-L10 and G30/S40-L20 samples, which exhibit a denser microstructure with fewer microcracks, resulting from the effective activation of silica and alumina from GBFS and silica fume. Fine aggregates and binder phases are well-integrated, forming a compact matrix. Figure 14-d, the SEM image of G30/S30-L30, shows moderate densification with isolated microcracks, reflecting balanced reactivity and structural integrity. G30/S20-L40 and G30/S10-L50 in Figures 14-e and 14-f increasing quick lime content leads to a less uniform matrix, with visible microcracks and voids due to shrinkage. Figure 14-g of G30/S0-L60 highlights the least compact structure with abundant porosity, reflecting over-reliance on lime, which disrupts the geopolymer network.
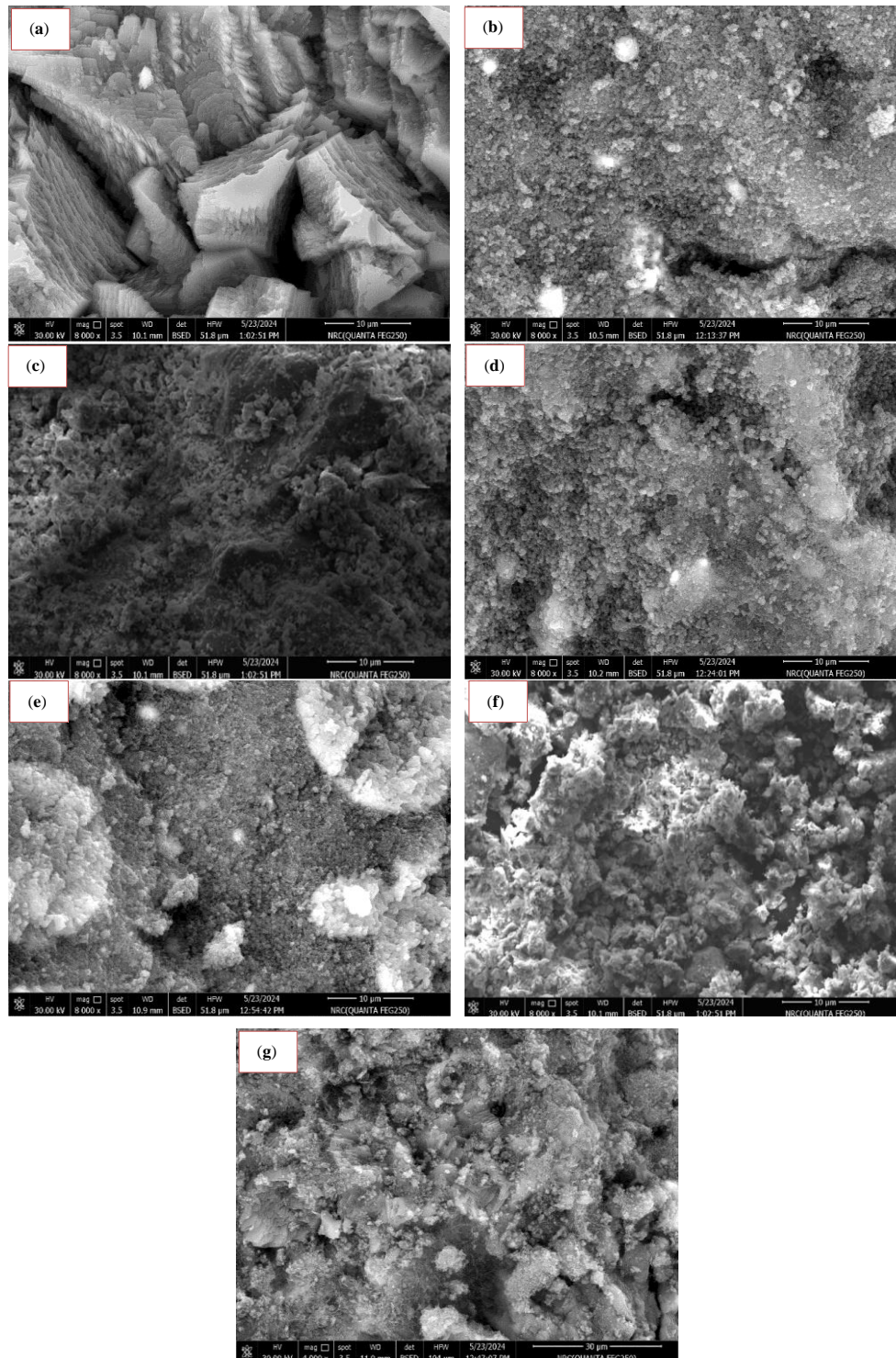

Figure 17. SEM images of alkali-activated mortar: (a) GB/S60-L0, (b) G30/S50-L10, (c) G30/S40-L20, (d) G30/S30-L30, (e) G30/S20-L40, (f) G30/S10-L50 and (g) G30/S0-L60

In addition, the SEM analysis provides detailed insights into the microstructural characteristics of mortar samples prepared using alkaline-activated geopolymer binders, highlighting the influence of binder composition on the morphology, compactness, and defect distribution in the matrix. Figure 14a, corresponding to the GB/S60-L0 sample, reveals a porous structure with significant voids. This porosity is primarily attributed to insufficient geo-polymerization caused by the low availability of reactive silica and alumina, which are critical for forming the dense C-S-H gel network. The lack of effective binding phases results in a weaker, less cohesive structure. In contrast, Figures 14b and 14c, representing G30/S50-L10 and G30/S40-L20 samples, showcase a denser and more compact microstructure with a notable reduction in microcracks. This improvement arises from the synergistic activation of silica and alumina sourced from granulated blast furnace slag (GBFS) and silica fume (SF). The well-integrated fine aggregates and binder phases in these samples create a uniform matrix with enhanced mechanical integrity.

Figure 14d, depicting G30/S30-L30, demonstrates moderate densification accompanied by isolated microcracks. The balanced reactivity of this composition supports adequate structural integrity but hints at localized areas of shrinkage. Figures 14e and 14f, for G30/S20-L40 and G30/S10-L50, respectively, highlight the adverse effects of increasing quick lime content. Higher lime levels lead to a heterogeneous matrix with visible microcracks and voids, reflecting shrinkage stresses and disruption of the geopolymer network. Finally, Figure 14g, showing G30/S0-L60, illustrates a highly porous and fragmented microstructure. The over-reliance on quick lime results in poor polymerization efficiency and structural instability, undermining the binder's overall performance. These observations underscore the importance of tailored binder compositions to achieve optimal microstructural and mechanical properties in geopolymer systems.

Previous research evaluating alkaline-activated geopolymer binders using RCA and industrial by-products demonstrated significant variations in mechanical performance. For instance, a study found that binders incorporating 30% fly ash, and 20% quick lime achieved compressive strengths of up to 35 MPa at 28 days [23]. Similarly, research highlighted the importance of silica fume, with mixtures containing 40% silica fume and 30% GGBFS achieving flexural strengths of 4.2 MPa [11]. Formulations with 40% RCA and red brick powder produced a denser microstructure, enhancing tensile strength by 18% compared to traditional mixes [4]. Another study emphasized that adding 50% GGBFS with 10% quick lime resulted in improved compressive strength but led to shrinkage-related microcracks [36].

Advances in durability assessments revealed critical influences of binder composition. An investigation indicated that 30% GGBFS with 20% quick lime reduced water absorption by 15% due to enhanced geopolymer gel formation [12]. In contrast, a different study noted that over-reliance on lime (above 40%) led to increased porosity and reduced durability under sulfate attack [55]. SEM analysis of mixtures with 50% silica fume demonstrated compact interfacial transition zones with minimal microcracks, improving freeze-thaw resistance by 20% [23]. A study confirmed that optimized blends with 30% RCA and industrial by-products formed a cohesive matrix with fewer voids, resulting in superior long-term performance [4, 52].

Accordingly, sustainability and cost-effectiveness were focal points in these studies. A study reported that replacing 40% of natural aggregates with RCA decreased overall material costs by 25% while maintaining satisfactory mechanical properties [26]. Different research highlighted the potential of red brick powder, which reduced reliance on imported materials and lowered production emissions by 18% [13, 56]. A comparative study concluded that the integration of industrial by-products could reduce carbon emissions by up to 30%, aligning with global sustainability goals [1, 2, 54]. Also, it was evident that geopolymer binders incorporating RCA offered a promising pathway to sustainable construction, with a 35% reduction in landfill waste and enhanced resource efficiency [36, 56].

4. Conclusions

The study demonstrated that geopolymer binders incorporating recycled concrete aggregate (RCA) and industrial by-products such as granulated blast furnace slag (GBFS), silica fume (SF), red brick powder (RBP), and quick lime (QL) provide viable alternatives to traditional cement. Optimal combinations of these materials result in improved mechanical properties, including compressive and flexural strength, as well as enhanced microstructural integrity.

- The performance of geopolymer binders strongly depends on the proportions of the alternative cementitious materials. Mixtures with balanced amounts of GBFS, SF, and RBP exhibited superior strength and durability, while excessive quick lime content led to porosity and reduced performance. This highlights the importance of tailoring material proportions to achieve desirable mechanical and microstructural properties.

- The findings underscore the potential of using RCA and industrial by-products to produce sustainable and environmentally friendly construction materials. These alternatives not only reduce reliance on conventional cement but also promote waste utilization, contributing to a circular economy in the construction industry.

- The setting times of geopolymer binders are significantly influenced by the composition of alternative cementitious materials, with GB/S60-L0 exhibiting the longest times (160 minutes initial, 260 minutes final) due to the slower reaction kinetics of high silica fume content, while G30/S0-L60 showed the shortest times (130 minutes initial, 217 minutes final) due to the acceleration effect of increased quick lime content.

- The results demonstrate that higher quick lime content enhances alkalinity, promoting faster geopolymer gelation and reducing setting times, while high silica fume content delays the process by requiring extended dissolution periods, consistent with findings in existing literature.

- The mix composition significantly influences flexural strength, with G30/S40-L20 achieving the highest performance (3.56 MPa at 7 days, 4.24 MPa at 56 days) due to the balanced proportions of SF and RBP, which enhance geo-polymerization and structural integrity, while excessive quick lime content in mixes like G30/S0-L60 results in reduced strength and microstructural compromise.

- Over time, the Control mix improved flexural strength to 4.75 MPa at 56 days, but optimized blends like G30/S40-L20 demonstrated potential for enhanced long-term tensile resistance, emphasizing the importance of carefully balancing binder ingredients to achieve durable and high-strength geopolymer matrices.

- The microstructural analysis revealed that binder composition significantly influences mortar compactness, with optimal mixtures (e.g., G30/S50-L10 and G30/S40-L20) exhibiting denser, well-integrated matrices and fewer microcracks due to effective activation of silica and alumina from GBFS and silica fume.

- Excessive quick lime content (e.g., G30/S0-L60) leads to poor microstructural integrity characterized by abundant porosity and disrupted geopolymer networks, highlighting the need for balanced binder formulation to ensure durability.

Also, further research is recommended to optimize geopolymer formulations for diverse environmental conditions and to investigate the long-term durability of these binders. Expanding the use of alternative activators and exploring other industrial by-products could further enhance the applicability of geopolymer technology in construction.

5. Declarations

5.1. Author Contributions

Conceptualization, M.S., T.I.S., and A.A.A.S.; methodology, W.F.E., M.S., and T.I.S.; formal analysis, M.S. and A.A.A.S.; data curation, W.F.E., R.S.A., and T.I.S.; writing—original draft preparation, A.A.A.S. and R.S.A.; writing—review and editing, R.S.A. and A.A.A.S.; supervision, T.I.S. and R.S.A. All authors have read and agreed to the published version of the manuscript.

5.2. Data Availability Statement

The data presented in this study are available on request from the corresponding author.

5.3. Funding and Acknowledgments

5.4. Conflicts of Interest

The authors declare no conflict of interest.

6. References

[1] John, S. K., Nadir, Y., & Girija, K. (2021). Effect of source materials, additives on the mechanical properties and durability of fly ash and fly ash-slag geopolymer mortar: A review. Construction and Building Materials, 280, 122443. doi:10.1016/j.conbuildmat.2021.122443.

[2] Chen, K., Wu, D., Yi, M., Cai, Q., & Zhang, Z. (2021). Mechanical and durability properties of metakaolin blended with slag geopolymer mortars used for pavement repair. Construction and Building Materials, 281, 122566. doi:10.1016/j.conbuildmat.2021.122566.

[3] Poornima, N., Katyal, D., Revathi, T., Sivasakthi, M., & Jeyalakshmi, R. (2021). Effect of curing on mechanical strength and microstructure of fly ash blend GGBS geopolymer, Portland cement mortar and its behavior at elevated temperature. Materials Today: Proceedings, 47, 863–870. doi:10.1016/j.matpr.2021.04.087.

[4] Singh, N. B., & Middendorf, B. (2020). Geopolymers as an alternative to Portland cement: An overview. Construction and Building Materials, 237, 1–15. doi:10.1016/j.conbuildmat.2019.117455.

[5] Matsimbe, J., Dinka, M., Olukanni, D., & Musonda, I. (2024). Performance evaluation and mix design of ambient-cured fly ash-phosphogypsum blended geopolymer paste and mortar. Results in Engineering, 24, 103280. doi:10.1016/j.rineng.2024.103280.

[6] Hwalla, J., El-Hassan, H., El-Mir, A., Assaad, J. J., & El-Maaddawy, T. (2024). Development of geopolymer and cement-based shotcrete mortar: Impact of mix design parameters and spraying process. Construction and Building Materials, 449, 138457. doi:10.1016/j.conbuildmat.2024.138457.

[7] Ghanim, H. A. A. E., Alengaram, U. J., Bunnori, N. M., & Ibrahim, M. S. I. (2025). Innovative in-house sodium silicate derived from coal bottom ash and its impact on geopolymer mortar. Journal of Building Engineering, 99, 111428. doi:10.1016/j.jobe.2024.111428.

[8] Bezabih, T., Sinkhonde, D., & Mirindi, D. (2025). On the surface roughness properties of fly ash-based geopolymer mortars with teff straw ash from the image analysis viewpoint. Green Technologies and Sustainability, 3(1), 100127. doi:10.1016/j.grets.2024.100127.

[9] Ardhira, P. J., Shukla, S. K., & Sathyan, D. (2024). Synthesis of geopolymer mortar from biomass ashes and forecasting its compressive strength behaviour. Case Studies in Construction Materials, 21, 3581. doi:10.1016/j.cscm.2024.e03581.

[10] Rezzoug, A., Leklou, N., Ayed, K., & Maryam, H. (2024). Enhancing geopolymer mortars for environmental sustainability: A novel approach using frits and ceramic waste. Next Research, 1(2), 100024. doi:10.1016/j.nexres.2024.100024.

[11] Chowdhury, S., Mohapatra, S., Gaur, A., Dwivedi, G., & Soni, A. (2021). Study of various properties of geopolymer concrete – A review. Materials Today: Proceedings, 46, 5687–5695. doi:10.1016/j.matpr.2020.09.835.

[12] Chen, Y., Zou, C., Yeo, J. S., Lin, J., Tan, T. H., & Mo, K. H. (2025). Valorization of high-volume crushed waste glass as fine aggregate in foamed geopolymer. Case Studies in Construction Materials, 22, 4202. doi:10.1016/j.cscm.2025.e04202.

[13] Sontia Metekong, J. V., Kaze, C. R., Deutou, J. G., Venyite, P., Nana, A., Kamseu, E., Melo, U. C., & Tatietse, T. T. (2021). Evaluation of performances of volcanic-ash-laterite based blended geopolymer concretes: Mechanical properties and durability. Journal of Building Engineering, 34, 101935. doi:10.1016/j.jobe.2020.101935.

[14] Wang, T., Fan, X., & Gao, C. (2024). Strength, pore characteristics, and characterization of fly ash-slag-based geopolymer mortar modified with silica fume. Structures, 69, 107525. doi:10.1016/j.istruc.2024.107525.

[15] Kogbara, R. B., Al-Zubi, A., & Masad, E. A. (2024). Dataset on early-age strength of ambient-cured geopolymer mortars from waste concrete and bricks with different alkaline activators. Data in Brief, 56, 110800. doi:10.1016/j.dib.2024.110800.

[16] Çelikten, S., Bayer Öztürk, Z., & Atabey, İ. İ. (2024). High-temperature resistance of ceramic sanitaryware waste and fly ash-based geopolymer and hybrid geopolymer mortars produced at ambient curing conditions. Construction and Building Materials, 446, 137990. doi:10.1016/j.conbuildmat.2024.137990.

[17] Mahmood, A. H., Foster, S. J., & Castel, A. (2021). Effects of mixing duration on engineering properties of geopolymer concrete. Construction and Building Materials, 303(April), 124449. doi:10.1016/j.conbuildmat.2021.124449.

[18] Rezzoug, A., Ayed, K., & Leklou, N. (2024). Thermal, mechanical and microstructural properties of geopolymer mortars derived from ceramic sanitary-ware wastes: Pathway to net zero emission. Ceramics International, 50(24), 55535-55545. doi:10.1016/j.ceramint.2024.10.414.

[19] Alharbi, Y. R., & Albidah, A. (2024). Synthesis of geopolymer mortar incorporating date palm ash. Construction and Building Materials, 449, 138512. doi:10.1016/j.conbuildmat.2024.138512.

[20] Rashad, A. M., Essa, G. M. F., Morsi, W. M., & Fahmy, E. A. (2024). Calcium nitrate as a modifier agent for metakaolin-based geopolymer mortar. Construction and Building Materials, 456, 139199. doi:10.1016/j.conbuildmat.2024.139199.

[21] Zhang, X., Li, H., Wang, H., Yan, P., Shan, L., & Hua, S. (2024). Properties of RCA stabilized with alkali-activated steel slag based materials in pavement base: Laboratory tests, field application and carbon emissions. Construction and Building Materials, 411, 134547. doi:10.1016/j.conbuildmat.2023.134547.

[22] Ariyadasa, P. W., Manalo, A. C., Lokuge, W., Aravinthan, V., Pasupathy, K., & Gerdes, A. (2024). Bond performance of fly ash-based geopolymer mortar in simulated concrete sewer substrate. Construction and Building Materials, 446, 137927. doi:10.1016/j.conbuildmat.2024.137927.

[23] Jain, S., Banthia, N., & Troczynski, T. (2022). Leaching of immobilized cesium from NaOH-activated fly ash-based geopolymers. Cement and Concrete Composites, 133, 104679. doi:10.1016/j.cemconcomp.2022.104679.

[24] Mohana, R., & Bharathi, S. M. L. (2024). Assessment on the mesh and mortar effect of the impact resistant nano fly ash based geopolymer ferrocement panels using rubber and plastic aggregates. Structures, 68, 107147. doi:10.1016/j.istruc.2024.107147.

[25] Huang, W., & Wang, H. (2024). Formulation development of metakaolin geopolymer with good workability for strength improvement and shrinkage reduction. Journal of Cleaner Production, 434, 140431. doi:10.1016/j.jclepro.2023.140431.

[26] Zhang, X., Bai, C., Qiao, Y., Wang, X., Jia, D., Li, H., & Colombo, P. (2021). Porous geopolymer composites: A review. Composites Part A: Applied Science and Manufacturing, 150, 106629. doi:10.1016/j.compositesa.2021.106629.

[27] Mohammadinia, A., Arulrajah, A., D'Amico, A., & Horpibulsuk, S. (2018). Alkali-activation of fly ash and cement kiln dust mixtures for stabilization of demolition aggregates. Construction and Building Materials, 186, 71–78. doi:10.1016/j.conbuildmat.2018.07.103.

[28] Damrongwiriyanupap, N., Wachum, A., Khansamrit, K., Detphan, S., Hanjitsuwan, S., Phoo-ngernkham, T., Sukontasukkul, P., Li, L. yuan, & Chindaprasirt, P. (2022). Improvement of recycled concrete aggregate using alkali-activated binder treatment. Materials and Structures/Materiaux et Constructions, 55(1), 1–20. doi:10.1617/s11527-021-01836-1.

[29] Yang, Z., Zhu, H., Zhang, B., Dong, Z., & Zhang, G. (2024). Fracture characteristics and microscopic mechanism of slag-based marine geopolymer mortar prepared with seawater and sea-sand. Construction and Building Materials, 450, 138561. doi:10.1016/j.conbuildmat.2024.138561.

[30] El Abd, A., Taman, M., Behiry, R. N., El-Naggar, M. R., Eissa, M., Hassan, A. M. A., Bar, W. A., Mongy, T., Osman, M., Hassan, A., Nabawy, B. S., & Rayan, A. M. (2024). Neutron imaging of moisture transport, water absorption characteristics and strength properties for fly ash/slag blended geopolymer mortars: Effect of drying temperature. Construction and Building Materials, 449, 138436. doi:10.1016/j.conbuildmat.2024.138436.

[31] Irum, S., & Shabbir, F. (2024). Performance of fly ash/GGBFS based geopolymer concrete with recycled fine and coarse aggregates at hot and ambient curing. Journal of Building Engineering, 95, 110148. doi:10.1016/j.jobe.2024.110148.

[32] Cheah, C. B., Tan, L. E., & Ramli, M. (2021). Recent advances in slag-based binder and chemical activators derived from industrial by-products – A review. Construction and Building Materials, 272, 121657. doi:10.1016/j.conbuildmat.2020.121657.

[33] Marathe, S., Sheshadri, A., & Sadowski, Ł. (2024). Agro-industrial waste utilization in air-cured alkali-activated pavement composites: Properties, micro-structural insights and life cycle impacts. Cleaner Materials, 14, 100281. doi:10.1016/j.clema.2024.100281.

[34] Tejas, S., & Pasla, D. (2024). Influence of agricultural waste ash on the mechanical strength of alkali-activated slag recycled aggregate concrete from a microstructural perspective. Innovative Infrastructure Solutions, 9(8), 335. doi:10.1007/s41062-024-01651-x.

[35] Xiaoshuang, S., Yanpeng, S., Jinqian, L., Yuhao, Z., & Ruihan, H. (2024). Preparation and performance optimization of fly ash-slag- red mud based geopolymer mortar: Simplex-centroid experimental design method. Construction and Building Materials, 450, 138573. doi:10.1016/j.conbuildmat.2024.138573.

[36] Huang, X., Tian, Y., Jiang, J., Lu, X., He, Z., & Jia, K. (2024). Mechanical properties and enhancement mechanism of iron ore tailings as aggregate for manufacturing ultra-high performance geopolymer concrete. Construction and Building Materials, 439, 137362. doi:10.1016/j.conbuildmat.2024.137362.

[37] Uğurlu, A. İ., Karakoç, M. B., & Özcan, A. (2021). Effect of binder content and recycled concrete aggregate on freeze-thaw and sulfate resistance of GGBFS based geopolymer concretes. Construction and Building Materials, 301, 124246. doi:10.1016/j.conbuildmat.2021.124246.

[38] Reddy, R.K., Yaragal, S. C., & Sagar Srinivasa, A. (2023). One-part eco-friendly alkali-activated concrete – An innovative sustainable alternative. Construction and Building Materials, 408, 133741. doi:10.1016/j.conbuildmat.2023.133741.

[39] Udhaya Kumar, T., & Vinod Kumar, M. (2020). Investigation on mechanical properties of geopolymer aggregate concrete. Materials Today: Proceedings, 43, 1220–1225. doi:10.1016/j.matpr.2020.08.758.

[40] Nikmehr, B., Kafle, B., & Al-Ameri, R. (2024). A review of the advanced treatment techniques for enriching the recycled concrete aggregates for recycled-based concrete: economic, environmental and technical analysis. Smart and Sustainable Built Environment, 13(3), 560–583. doi:10.1108/SASBE-11-2022-0243.

[41] Hassani, A., & Kazemian, F. (2024). Investigating geopolymer mortar incorporating industrial waste using response surface methodology: A sustainable approach for construction materials. Case Studies in Construction Materials, 21, 3609. doi:10.1016/j.cscm.2024.e03609.

[42] Shahid, M. J., Khan, H. A., Khan, M. Z. N., Ahmad, J., & Abdullah, M. (2024). Optimization of an alkali activator solution to enhance the performance of roller-compacted concrete for pavements (RCCP). International Journal of Pavement Engineering, 25(1), 2318609. doi:10.1080/10298436.2024.2318609.

[43] Kumar, C. B. (2022). Performance Evaluation of Ferrochrome ASH Based Alkali Activated Slag Mortars. Ph.D. Thesis, National Institute of Technology Karnataka, Mangaluru, India.

[44] ASTM C33/C33M-18. Standard Specification for Concrete Aggregates. ASTM International, Pennsylvania, United States. doi:10.1520/C0033_C0033M-18.

[45] ASTM C150/C150M-19. (2019). Standard Specification for Portland Cement. ASTM International, Pennsylvania, United States. doi:10.1520/C0150_C0150M-19.

[46] ASTM C1602/C1602M-22. (2022). Standard Specification for Mixing Water Used in the Production of Hydraulic Cement Concrete. ASTM International, Pennsylvania, United States. doi:10.1520/C1602_C1602M-22.

[47] ASTM C191-21. (2021). Standard Test Methods for Time of Setting of Hydraulic Cement by Vicat Needle. ASTM International, Pennsylvania, United States. doi:10.1520/C0191-21.

[48] ASTM C1437-20. (2020). Standard Test Method for Flow of Hydraulic Cement Mortar. ASTM International, Pennsylvania, United States. doi:10.1520/C1437-20.

[49] ASTM C109/C109M-20. (2020). Standard Test Method for Compressive Strength of Hydraulic Cement Mortars (Using 2-in. or [50-mm] Cube Specimens). ASTM International, Pennsylvania, United States. doi:10.1520/C0109_C0109M-20.

[50] ASTM C1709-18. (2023). Standard Guide for Evaluation of Alternative Supplementary Cementitious Materials (ASCM) for Use in Concrete. ASTM International, Pennsylvania, United States. doi:10.1520/C1709-18.

[51] BS EN 1015. (2019). Methods of test for mortar for masonry - Determination of flexural and compressive strength of hardened mortar. British Standard Institute (BSI), London, United Kingdom.

[52] Anju, M. J., Beulah, M., & Varghese, A. (2024). Review of Geopolymer Composites Synthesized Using Different Industrial By-products. International Journal of Pavement Research and Technology. doi:10.1007/s42947-024-00446-8.

[53] Poletanovic, B., Kopecsko, K., & Merta, I. (2024). Fibre hornification improves the long-term properties of hemp fibre-reinforced fly ash-based geopolymer mortar. Construction and Building Materials, 446, 137957. doi:10.1016/j.conbuildmat.2024.137957.

[54] Singh, R. P., Vanapalli, K. R., Jadda, K., & Mohanty, B. (2024). Durability assessment of fly ash, GGBS, and silica fume based geopolymer concrete with recycled aggregates against acid and sulfate attack. Journal of Building Engineering, 82, 108354. doi:10.1016/j.jobe.2023.108354.

[55] Rahman, S. S., & Khattak, M. J. (2023). Feasibility of Reclaimed Asphalt Pavement Geopolymer Concrete as a Pavement Construction Material. International Journal of Pavement Research and Technology, 16(4), 888–907. doi:10.1007/s42947-022-00169-8.

[56] Walkley, B., Ke, X., Hussein, O. H., Bernal, S. A., & Provis, J. L. (2020). Incorporation of strontium and calcium in geopolymer gels. Journal of Hazardous Materials, 382, 121015. doi:10.1016/j.jhazmat.2019.121015.